Release of methane from Bering Sea sediments during the last glacial period

Final Scientific Report

Reporting period: October 1, 2005 to November 30, 2007

Principal Authors:
Mea S. Cook
Lloyd D. Keigwin

Date report issued: February 29, 2008

DOE award number: DE-FC26-05NT42665

Mea S. Cook
University of California
Ocean Sciences Department
1156 High Street
Santa Cruz, CA 95062

Lloyd D. Keigwin
Woods Hole Oceanographic Institution
Mail Stop #8
Woods Hole, MA 02543

DISCLAIMER

ABSTRACT

Several lines of evidence suggest that during times of elevated methane flux the sulfate-methane transition zone (SMTZ) was positioned near the sediment-water interface. We studied two cores (from 700 m and 1457 m water depth) from the Umnak Plateau region. Anomalously low d13C and high d18O in benthic and planktonic foraminifera in these cores are the consequence of diagenetic overgrowths of authigenic carbonates. There are multiple layers of authigenic-carbonate-rich sediment in these cores, and the stable isotope compositions of the carbonates are consistent with those formed during anaerobic oxidation of methane (AOM). The carbonate-rich layers are associated with biomarkers produced by methane-oxidizing archaea, archaeol and glyceryl dibiphytanyl glyceryl tetraether (GDGT). The d13C of the archaeol and certain GDGTs are isotopically depleted. These carbonate- and AOM-biomarker-rich layers were emplaced in the SMTZ during episodes when there was a high flux of methane or methane-rich fluids upward in the sediment column. The sediment methane in the Umnak Plateau region appears to have been very dynamic during the glacial period, and interacted with the ocean-atmosphere system at millennial time scales. The upper-most carbonate-rich layers are in radiocarbon-dated sediment deposited during interstadials 2 and 3, 28-20 ka, and may be associated with the climate warming during this time.

TABLE OF CONTENTS

EXECUTIVE SUMMARY

The stability of sedimentary methane hydrates over glacial-interglacial time periods is not well known. Today, flux of methane to the atmosphere from seafloor hydrates is far smaller than the flux from other natural sources. However, it is hypothesized by Kennett et al. (2003) that during times of rapid climate warming in the last glacial period, methane flux from the seafloor to the atmosphere was a significant contributer to global warming.

The evidence supporting Kennett's hypothesis comes primarily from the Santa Barbara Basin, where in a sediment core there are carbon isotope data from the seafloor and sea surface (benthic and planktonic foraminifera, respectively) that suggest that there were repeated occurrences of methane release from a local source. Hinrichs et al (2003) extracted lipid biomarkers from the same sediment core and found compounds specific to methane-oxidizing archaea during two climate warming events.

However, isotopic studies of methane from fossil air samples recovered from ice cores do not support the hypothesis that methane hydrates were responsible for the entire rise in atmospheric methane concentrations during the climate events. Sowers (2006) and Schaefer et al. (2006) measured the hydrogen isotopes and carbon isotopes, respectively, of atmospheric methane during warm climate transitions. These studies do not exclude the possibility that methane hydrates contributed to part of the rise in atmospheric methane observed during these time periods.

There are several other locations around the Atlantic and Pacific where there is evidence of methane flux to the seafloor during the last glacial period. However, since this time period is mostly out of the range of radiocarbon dating, correlating these observations to the climate events is not possible at present. In addition, none of these records show episodes of methane flux that are as numerous and persistent as the warm climate events that occurred during the last glacial period.

In this project, we studied the inorganic and organic geochemistry of the glacial sediments from two cores from the southeast Bering Sea. We observed geochemical signatures of intense upward flux of methane to the seafloor. These episodes occurred repeatedly during the last glacial period, and have similar duration and timing as the warm climate events that are associated with atmospheric methane rise.

We found layers of sediment rich in authigenic carbonate minerals in two sediment cores from the southeast Bering Sea. These minerals have low ^{13}C-^{12}C ratios and high ^{18}O-^{16}O ratios, which is consistent with authigenic carbonates that form in modern active methane seep areas. We then extracted lipid biomarkers from the sediments containing the authigenic carbonates. We found lipids that are unique to methane-oxidizing archaea, and which had the charactistically low ^{13}C-^{12}C ratio expected in methanotropic microbes.

We also studied the distribution of benthic foraminifer species in these sediments. We hypothesized that if the methane flux were high enough, the methane would escape out of

the sediments into the water column. In addition, the authigenic carbonates and lipid biomarkers would be emplaced at the seafloor in recently deposited sediment, and the benthic foraminifera living on the seafloor would react to the methane flux and affect the species distribution. We found that the population shifted in sync with the occurrence of authigenic carbonates and biomarkers.

With radiocarbon dating, we found that the episodes of authigenic carbonates occur with similar duration and timing as the warm climate events of the last glacial period. The precision of the radiocarbon dates is not good enough to tell whether the episodes in our sediment core are in phase or out of phase with the climate events. However, our data do show that sedimentary methane in the Bering Sea was very dynamic during the last glacial period. It interacted with the ocean-atmosphere system on the same time scale as rapid climate events.

These findings are significant because for the first time outside the Santa Barbara Basin, we have observed a marine methane reservoir that is dynamically interacting with the ocean-atmosphere system during the last glacial period. This is strong support for the idea that sedimentary methane may be an important source of greenhouse gas to the atmosphere during times of rapid climate warming in the past.

1. INTRODUCTION

Though methane is a relatively minor component of the atmosphere (760 ppbv pre-industrial concentration), it is an important greenhouse gas. Methane causes 26 times the warming as the same mass of carbon dioxide over 10 years (LELIEVELD et al., 1993).

1.1. The global methane budget

The modern-day flux of methane to the atmosphere is dominated by wetlands at 145 Tg/y (MIKALOFF FLETCHER et al., 2004). The flux from methane hydrates is 5 Tg/y and may seem small. However, there are large reservoirs of methane in sea-floor sediments and permafrost regions. The sizes of these reservoirs are not well known, but recent estimates include 500,000–2,500,000 Tg in the seafloor (MILKOV, 2004) and 400,000 Tg in permafrost (MACDONALD, 1990). Because of its sheer size, a perturbation in the methane hydrate reservoir has the potential to have a large influence on climate.

1.2. The climate influence of sedimentary methane

Release of methane from seafloor sediments is thought to be associated with climate changes in the past, including during the early Jurrasic (HESSELBO et al., 2000), the Paleocene-Eocene thermal maximum (DICKENS et al., 1995), and in the last glacial period (KENNETT et al., 2003). In the late Pleistocene, the atmospheric concentration of methane varied between 350 and 760 ppbv, or 1,100 and 2,200 Tg, where methane is high during warm interglacial periods, and low during cold glacial periods (CHAPPELLAZ et al., 1990).

During the last glacial period, there were millennial-scale climate shifts called Dansgaard-Oeschger (DO) events (JOHNSEN et al., 1992). The warm, interstadial, climate events are associated with elevated atmospheric methane concentrations (BLUNIER et al., 1998), which has been interpreted as higher methane flux from expanded wetlands during warm climate phases (CHAPPELLAZ et al., 1990). However, Kennett et al. (2003) have proposed that sedimentary methane hydrates could be a significant source of atmospheric methane during these climate events.

Evidence from marine sediments of methane flux from the seafloor during the late Quaternary include Santa Barbara Basin (HILL et al., 2006; HINRICHS et al., 2003; KENNETT et al., 2000), the Gulf of California (KEIGWIN, 2002), the Japan margin (HOSHIBA et al., 2006; UCHIDA et al., 2004), the Okhotsk Sea (LEMBKE et al., 2003), the Papua Gulf (DE GARIDEL-THORON et al., 2004), the Indonesian margin (WIEDICKE and WEISS, 2006), the Peru margin (WEFER et al., 1994), the east Greenland shelf (SMITH et al., 2001), the southwest Greenland Sea (MILLO et al., 2005), the Amazon Fan (MASLIN et al., 2004), and Blake Ridge (BHAUMIK and GUPTA, 2007).

1.3. Geochemical setting in seep environments, inorganic and organic

In modern methane seeps, there are commonly accumulations of carbonate minerals. These occur because a product of anaerobic methane oxidation is bicarbonate ion (HCO_3^-). A large flux of bicarbonate to the porewater from vigorous methane oxidation increases the alkalinity and causes supersaturation of a variety of carbonate minerals,

including high-Mg calcite, aragonite, and dolomite (Orphan et al., 2003). In addition, there is accumulation of biomass of the methane-oxidizing microbial community in the sediment.

In organic-carbon- (C_{org}) rich marine sediments, when more energetically favorable oxidants are depleted, C_{org} is reduced to methane by a consortium of archaea and bacteria by CO_2 reduction (CLAYPOOL and KAPLAN, 1974).

$$2CH_2O + 2H_2O \rightarrow 2CO_2 + 8(H)$$
$$CO_2 + 8(H) \rightarrow CH_4 + 2H_2O$$

The $\delta^{13}C$ of this biogenic methane is typically –110 to –50‰ because of strong kinetic fractionation during CO_2 reduction (WHITICAR et al., 1986). Biogenic methane will diffuse upward in the sediment column into the overlying sulfate reduction zone. In the presence of sulfate, methane is oxidized by syntropic anaerobic sulfate-reducing bacteria and archaea (ALPERIN and REEBURGH, 1984).

$$CH_4 + SO_4^{2-} \rightarrow 2HCO_3^- + HS^- + H_2O$$

with further fractionation of 2–14‰ (WHITICAR and FABER, 1986). A biomarker characteristic of anaerobic methane oxidation is archaeol (LANGWORTHY, 1986). All archaea produce glyceryl dibiphytanyl glyceryl tetraethers (GDGTs) as part of their cell membrane. Archaeol or GDGT from a methane-oxidizing archaea would have low $\delta^{13}C$ characteristic of anaerobic methane oxidation (WAKEHAM et al., 2003).

1.4. The purpose of this study

In cores from the southeast Bering Sea, we identified episodes during the last glacial period when authigenic carbonate minerals were emplaced within the sediment. We hypothesize that this was due to a significant flux of methane to the seafloor. We studied the stable isotopic composition of these authigenic minerals to see if it was consistent with origin in a methane-rich environment. We also extracted and studied lipid biomarkers from these episodes to deduce what microbial community was present in the sediments at the time. We also studied changes in the benthic foraminifer population assemblage to assess whether the high methane flux was occurring at the seafloor, indicating that the methane may have been escaping into the water column.

2. METHODS

Piston cores HLY02-02-51JPC (1467 m water depth) and HLY02-02-57JPC (700 m water depth) were collected in June, 2002, from the crest of the broad spur between the Bering and Bristol Canyons in the southeast Bering Sea (Figure 1). The cores were split lengthwise and stored at 5˚C. One-centimeter-thick samples were taken approximately every 8 cm from the coretop to 1192 cm in 51JPC and from the coretop to 1096 cm in 57JPC.

2.1. Micropaleontology

Sediment samples for foraminifer isotope analyses were oven dried at 50˚C, washed with tap water through a 63 μm sieve, then oven dried again. Planktonic foraminifer *Neogloboquadrina pachyderma* (sinistral) and benthic foraminifer *Uvigerina peregrina* were picked from the 150–250 μm and >250 μm size fractions, respectively. Without further cleaning, samples consisting of 8–10 *N. pachyderma* (s.) or a single *U. peregrina*

were analyzed on a Finnigan MAT253 mass spectrometer with a Kiel device. The $\delta^{18}O$ and $\delta^{13}C$ are reported relative to the VPDB standard following standard procedures (OSTERMANN and CURRY, 2000).

Benthic foraminifer species distribution was assessed by counting and identifying individuals in the >150 μm size fraction. Uncertainty of relative abundance was calculated as in Fatel & Taborda (2002).

Samples of *N. pachyderma* (s.) were submitted to the National Ocean Sciences Accelerator Mass Spectrometer Facility at WHOI for AMS ^{14}C analysis. The $\delta^{13}C$ was measured on an aliquot of each sample. The ^{14}C measurements (Table 1) were transformed to calendar ages using the Calib 5.0.1 software. We used the Intcal2004 calibration dataset (REIMER et al., 2004), and assumed that ΔR, the local anomaly of the age of surface water from the global mean, is constant at 400 y (COOK et al., 2005). This corresponds to a total reservoir correction, R, of 800 y with an uncertainty of $\sigma = 200$ y. For the ^{14}C measurements beyond the range of the Intcal2004 dataset, we found a calendar age by finding the intercept of the conventional ^{14}C age with a curve of ^{14}C age versus calendar age BP of the planktonic foraminifer *Globigerina bulloides* from Cariaco Basin (HUGHEN et al., 2004). This record is tuned to GRIP $\delta^{18}O$ of ice on the ss09sea age model (JOHNSEN et al., 2001). The simple depth-age models for these cores assume constant sediment accumulation rates between calibrated ^{14}C ages. We measured ^{14}C on samples of *N. pachyderma* (s.) from each core from which we knew there was significant overgrowth of authigenic minerals.

2.2. Lipid biomarkers

Sediment samples for lipid extraction were taken from the sediment cores in December, 2006. They were freeze-dried with a Martin Christ Alpha 1-4 freeze dryer, then homogenized with an agate mortar and pestle. Eight to 14 g of homogenized sediment were extracted with a mixture of dichloromethane and methanol (3:1 ratio) after addition of 20 μg of a recovery standard, 1-nonadecanol. The solvent was removed from the total lipid extract (TLE) under a stream of N_2 in a 35˚C water bath (Turbovap).

The *n*-hexane–soluble (maltene) fraction of the TLE was passed through a solid phase extraction column containing 500 mg aminopropyl-bonded silica (Supelco) with the following series of solvents in increasing polarity: 4 mL *n*-hexane, 6 mL *n*-hexane and dichloromethane (3:1 ratio), 7 mL dichloromethane and acetone (9:1 ratio), and 2% formic acid in dichloromethane (v/v).

All alcohol fractions were analyzed as their trimethylsilyl (TMS) derivatives in a Thermo Electron Trace gas chromatograph (GC) mass spectrometer (MS) with a DB-5MS fused-silica capillary column (30 m length, 0.25 mm inner diameter, 0.25 μm film thickness) using helium as the carrier gas. We used the following temperature program: injection at 60˚C, isothermal for 2 min, heat at 10˚C/min to 150˚C, heat at 4˚C/min to 320˚C, isothermal for 31.5 min. Compounds were identified based on their retention times and comparison of the mass spectra to published spectra. Compound-specific $\delta^{13}C$ measurements of derivatized alcohol fractions were performed on a Hewlett Packard

5890 gas chromatograph coupled to Finnigan MAT 252 MS via a Thermo Electron GCC-II combustion interface. The GC column and temperature program were the same as in the GC-MS. We corrected measured $\delta^{13}C$ for the contribution of TMS using the known $\delta^{13}C$ of the n-bis(trimethylsilyl)trifluoroacetamide reagent.

In order to study the constituent biphytanes of intact polar membrane lipids, we performed ether cleavage of an aliquot of the underivatized alcohol fraction after addition of 20 μg of a recovery standard, cholestane. The ether bonds in the sample were cleaved by reaction with hydrogen iodide at 110˚C for 4 hours. The iodide salts were reduced to hydrocarbons by reaction with $LiAlH_4$ under a nitrogen atmosphere at 110˚C for 3 hours. The hydrocarbon products were analyzed on the same GC-MS system described above, but with the following temperature program: injection at 60˚C, isothermal for 1 min, heat at 15˚C/min to 150˚C, heat at 4˚C/min to 310˚C, isothermal for 28 min. Compound-specific $\delta^{13}C$ measurements were performed on a Thermo Electron Trace GC coupled to a Thermo Electron Delta Plus XP MS via a Thermo Electron GCC-II combustion interface. The GC column and temperature program were the same as in the GC-MS.

3. RESULTS AND DISCUSSION

3.1. Foraminifer stable isotopes

In 51JPC, the Last Glacial Maximum (LGM) is at around 300 cm (Figure 2). In 57JPC, the sediment accumulation rate is lower during the deglaciation, so the LGM is at about 150 cm. The sediment accumulation rate during the glacial period is similar in both cores, at around 30 cm/ky.

During the glacial period in both cores, we find large negative excursions in $\delta^{13}C$ of both *N. pachyderma* (s.) (as low as –14‰) and *U. peregrina* (as low as –6.8‰) (Figure 2). The low $\delta^{13}C$ is associated with high $\delta^{18}O$. Upon visual inspection, the foraminifera in the samples with anomalous isotopic values appear yellowish (Figure 3), which we hypothesize is due to post-depositional overgrowths of authigenic carbonate minerals. We considered the composition of the samples we measured as a combination of foraminifer calcite and authigenic carbonates. The scatter of measurements in $\delta^{13}C$-$\delta^{18}O$ space would fall on a linear mixing curve between the compositions of primary test calcite and authigenic carbonate (NORRIS and DE VARGAS, 2000; SCHMIDT et al., 2002)

$$\delta^{18}O_{meas} = \delta^{18}O_{foram}\varphi + \delta^{18}O_{auth}(1-\varphi)$$
$$\delta^{13}C_{meas} = \delta^{13}C_{foram}\varphi + \delta^{13}C_{auth}(1-\varphi)$$

where φ is the fraction of the test that is composed of foraminifer calcite.

In Figure 4, *N. pachyderma* (s.) $\delta^{13}C$ less than –2‰ are circled, and a linear least-squares fit is applied through the circled points.

$$\delta^{18}O = -0.145\ \delta^{13}C + 3.33\ (n = 47;\ r^2 = 0.826;\ p < 10^{-4})$$

We can estimate the composition of the authigenic carbonate crust using the $\delta^{18}O$ and $\delta^{13}C$ measurements on two samples of *N. pachyderma* (s.), one with and one without overgrowth (Table 1). We assume that the difference in mass between the two samples from a constrained size fraction is due to the addition of authigenic carbonate to the

altered sample. Our estimate of the $\delta^{18}O$ and $\delta^{13}C$ of the authigenic carbonates are 6.5‰ and –23.4‰, respectively.

The estimate of $\delta^{18}O$ of authigenic carbonate is 1.6‰ higher than mean $\delta^{18}O$ of *U. peregrina* measured outside low $\delta^{13}C$ events in samples 450–750 cm in 51JPC. The higher $\delta^{18}O$ of the authigenic carbonate could be from 1) a change in porewater $\delta^{18}O$, 2) a thermodynamic effect, such as change in temperature, or a difference in the mineralogy between the overgrowth and the foraminifer calcite, and/or 3) a kinetic effect, where the [Mg] of the porewater and/or authigenic calcite affects growth rate and incorporation of oxygen isotopes (BERNER, 1980; TARUTANI et al., 1969). We think it's likely that the $\delta^{18}O$ we estimate for the authigenic carbonate minerals is a function of the mineralogy of the overgrowths, which may be composed of a mixture of aragonite, dolomite, and high-magnesium calcite (ORPHAN et al., 2004). Dolomite (FRITZ and SMITH, 1970)and high-Mg calcite (TARUTANI et al., 1969) have equilibrium values of $\delta^{18}O$ higher than calcite and can easily account for this difference.

The $\delta^{13}C$ we estimate for the authigenic carbonates is not low enough to require the presence of methane. We think that the porewater dissolved inorganic carbon at the time the authigenic minerals formed could have been a combination of carbon from seawater (+1 to –1‰), organic carbon (–22‰) (RAU et al., 1982), and carbon that is was product of methanotrophy (–110 to –50‰). Though the presence of authigenic carbonates alone suggests that there was a high methane flux upward in the sediment column, we need to turn to a more specific technique (biomarkers) to ascertain whether there was indeed methane present.

3.2. Benthic foraminifer species distribution

The benthic foraminifera are predominantly composed of 6 species, *U. peregrina*, *Nonionella* sp., *Islandella* sp., *Elphidium excavatum*, *Globobulimina affinis*, and *Buliminella* sp.. We made census counts of the benthic foraminifera during the three stratigraphically highest isotopic excursions in each core (Figure 5). During the isotopic excursions, the relative abundance of *Nonionella* sp. increases and the relative abundance of *U. peregrina* and *Islandella* sp. decrease. Since these changes in benthic foraminifer species distribution occur in the same depths as the occurrence of authigenic minerals, we hypothesize that the sulfate-methane transition zone was at the seafloor, altering the habitat of the benthic foraminifera while the authigenic minerals were emplaced.

3.3. Biomarkers

We performed extraction and identification of lipid biomarkers. Archaeol, a biomarker of archaea that perform anaerobic oxidation of methane, is present, but generally in very low concentrations. By examining the distribution of compounds in the samples, we discovered that the most degradation-susceptible compounds were absent, suggesting that these samples had already undergone significant degradation since core collection in 2002. This could explain why archeaol was not always present in samples that contained authigenic carbonates.

Since we could get very little isotopic data from our initial target biomarker, archeaol, we turned to another class of compounds, glyceryl dibiphytanyl glyceryl tetraethers (GDGTs), which are produced by all archaea, including planktonic archaea, those that live in the water column. Therefore we expect to find that the GDGTs in our samples are a mixture of planktonic archaea and the archaea that lived in the sediment. However, it has been found that oxic planktonic archaea tend to make GDGTs with acyclic, monocyclic, dicyclic or tricyclic biphytane chains, whereas archaea that perform anaerobic oxidation of methane produce GDGTs with acyclic and monocyclic biphytane chains (WAKEHAM et al., 2003).

For a series of samples, we isolated the alcohol fraction from the total lipid extract, which contained any archaeol and GDGTs from the samples. We then performed an ether cleavage reaction, which liberated phytanes from the archaeol in the sample and biphytanes from the GDGTs in the sample. We then measured the $\delta^{13}C$ of the phytane and biphytanes (Figure 6).

We find that the $\delta^{13}C$ of archaeol and phytane are as low as –80‰ in 51JPC, and as low as –40‰ in 57JPC. In these same samples, the $\delta^{13}C$ of monocyclic and acyclic biphytane are significantly lower. We interpret these results to mean that there was indeed an active microbial community performing anaerobic oxidation of methane in the sediments in each episode where authigenic minerals were emplaced.

The $\delta^{13}C$ depletion of these biomarkers occurs in sediments stratigraphically slightly below where authigenic carbonate minerals are present. This is consistent with a vertical flux of pore fluids, which would be the case if there was methane or methane-rich fluid advected upward in the sediment column. The methane-oxidizing microbial community would have been in the sulfate-methane transition zone, and their ^{13}C-depleted metabolic products, including HCO_3^-, would have been carried upward. The excess of HCO_3^- would have caused the supersaturation of pore fluids with respect to carbonate minerals and formed authigenic-carbonate-mineral rich layers of sediment slightly above the sulfate-methane transition zone.

3.4. The souce of methane

If the authigenic minerals are associated with a greater flux of methane to the surface sediments, this raises a quandary. The coring site of 51JPC is so cold and deep, that destabilization of methane hydrates at this site would require an unrealistic warming (15˚C) or sea-level drop (–1100 m). However, methane can be transported within the hydrate stability zone if (1) the concentration is not high enough to form hydrate or (2) there is a kinetic barrier to the formation of hydrate. Methane gas released into seawater (at pressure and temperature conditions within the hydrate stability zone) can form a crust of hydrate around the periphery of the bubble, isolating the gas in the interior of the bubble from the seawater, and slowing the hydrate formation (BREWER et al., 1998). The positive buoyancy of the bubble then would move it upward. In the Black Sea, there are active methane seeps observed within the hydrate stability zone (KLAUCKE et al., 2005).

The Bering Sea is in a seismically active area, and we speculate that seismic activity could have played a role in causing upward fluid flux in the region. For example, slow earthquakes in subduction zones have been linked to small changes in hydrostatic pressure caused by tides (LOWRY, 2006; RUBINSTEIN et al., 2008; SHEN et al., 2005). There were significant sea-level changes during the last glacial period, associated with the millennial-scale climate changes at the time (SIDDALL et al., 2003).

We also speculate that the sediments in the Bering Sea could be susceptible to fluid expulsion during a seismic event. The sediments in the Bering Sea are very rich in biogenic silica (diatoms) (TSUNOGAI et al., 1979), and when compacted, diatom tests spontaneously transform from opal A to opal CT, a reaction that liberates water and causes sediment compaction (WILLIAMS and CRERAR, 1985; WILLIAMS et al., 1984). The progression of the diagenetic front in silia-rich sediments can be responsible for signficiant overpressure in pore fluids, massive fluid expulsion, and in continental slope areas, slope failure, injectites, and canyon exfoliation (DAVIES and CLARK, 2006; DAVIES et al., 2006; MCHUGH et al., 1993).

We would have to carry out sediment modelling in order to ascertain whether these speculative mechanisms would be able to produce a significant flux of methane-bearing fluids, and also to estimate the magnitude of methane flux requried to explain our observations in the Bering Sea cores. We intend to pursue this avenue of work in the future.

3.5. Climate implications

According to the preliminary age model, the duration of each of the three episodes of low $\delta^{13}C$ was less than 1000 y, and the events appeared to be spaced greater than 1000 y apart. Though the age model is too preliminary to show if the events in the core coincide chronologically with DO events, they appear to have similar duration and timing. If these episodes coincide with DO events, then it supports the idea that sedimentary methane hydrates interact with the climate system on short timescales (KENNETT et al., 2003). However, the mechanism proposed by Kennett et al (2003) cannot explain the presence of methane in coring sites that is as deep and cold as 51JPC and 57JPC.

4. CONCLUSIONS

We find evidence of authigenic carbonates with low $\delta^{13}C$ and high $\delta^{18}O$ which occur during the last glacial period two sediment cores from 700 m and 1500 m water depth in the Umnak Plateau region. These overgrowths may be associated with vigorous anaerobic oxidation of methane caused by high flux of methane or methane-bearing fluids upward in the sediment column. In the authigenic carbonate-rich sediments, we found lipid biomarkers associated with anaerobic methanotropic archaea, confirming that these inorganic and organic geochemical markers formed in sediment within an ancient sulfate-methane transition zone, when methane flux was high. We found that benthic foraminifer populations changed in synch with the fossil sulfate-methane transition zones, which is consistent with the zone being located at the seafloor, and methane being released into the water column. According to a radiocarbon-based age model, the episodes of methane flux lasted ~1000 y each, and occurred every few thousand years,

the same duration and timing as warm global climate events that occurred during the last glacial period. We conclude that the sedimentary methane reservoir in the Umnak Plateau region appears to be very dynamic, and interacted with the ocean system on millennial time scales during the last glacial period.

5. GRAPHICAL MATERIALS LIST

Figure 1. Map of the study area. Thin black lines are 1000 m countours.

Figure 2. The $\delta^{13}C$ stratigraphies of cores 57JPC (top) and 51JPC (bottom). The black and green lines are of planktonic (*N. pachyderma* (s.)) and benthic (*U. peregrina*) foraminifer samples, respectively. The triangles are locations of radiocarbon dates. The Last Glacial Maximum is at 150 cm in 57JPC, and at 300 cm in 51JPC. The low $\delta^{13}C$ excursions occur during the last glacial period.

Figure 3. Photographs of N. pachyderma (s.) (top) and U. peregrina (bottom) from samples with ordinary late Pleistocene isotopic values (left) and from samples with anomalous isotopes (right).

Figure 4. The estimate of the $\delta^{13}C$ and $\delta^{18}O$ of the authigenic carbonate minerals. The black and red dots are from 51JPC and are of planktonic (*N. pachyderma* (s.)) and benthic (*U. peregrina*) foraminifer samples, respectively. The circled planktonic data from 51JPC have $\delta^{13}C$ lower than –2, and are considered isotopically anomalous. They are used to calculate the least-squares best-fit line (dashed black line) that fits our simple linear mixing model with two end members (see text). Our estimate of the composition of the authigenic end member using this mixing model is marked with the blue star. The red dashed line connects the authigenic end member with the mean glacial benthic end member. The blue and cyan dots are from 57JPC and are of planktonic (*N. pachyderma* (s.)) and benthic (*U. peregrina*) foraminifer samples, respectively. The authigenic end member in both coring locations appears to have a very similar composition.

Figure 5. The benthic foraminifer relative abundances (bottom panels) for the three stratigraphically highest isotopic events in core 51JPC (left) and 57JPC (right). The data for *U. peregrina*, *Nonionella* sp., and *Islandella* sp. are plotted in blue, black, and red respectively. For reference, the $\delta^{13}C$ stratigraphies are plotted in the top panels, where the black and green lines are the planktonic (*N. pachyderma* (s.)) and benthic (*U. peregrina*) foraminifer samples, respectively.

Figure 6. Lipid biomarker data from 51JPC (left) and 57JPC (right). On the bottom panels are the $\delta^{13}C$ in the two cores, where the black and green lines are the planktonic (*N. pachyderma* (s.)) and benthic (*U. peregrina*) foraminifer samples, respectively. In the top panels are the concentration of archaeol (a biomarker of methane-oxidizing archaea) in the cores. In most cases, not enough archaeol was present to measure $\delta^{13}C$ on that biomarker. In the middle panel are the $\delta^{13}C$ of archaeol (when possible), phytane (an ether-cleavage product of archaeol), and a series of biphytanes (ether-cleavage product of GDGTs, molecues from archeal cell walls). The $\delta^{13}C$ of archaeol, phytane, and constitutent biphytanes of GDGTs are significantly lower in horizons where there are authigenic minerals present.

Figure 7. Isotopic data from plotted versus time. The black and green lines are of planktonic (*N. pachyderma* (s.)) and benthic (*U. peregrina*) foraminifer samples,

respectively. The age model is based on radiocarbon dates (triangles) and a tie point between 51JPC and 57JPC (*) based on magnetic susceptibility and density data (not shown). The top panel is $\delta^{18}O$ of ice from the GISP2 ice core (GROOTES and STUIVER, 1997). This is a surface air temperature proxy, where lower $\delta^{18}O$ is lower temperature, and higher $\delta^{18}O$ is higher temperature. The next panel shows the methane concentration from fossil air from Greenland and Antarctica (pale blue and dark blue, respectively) (BLUNIER et al., 1998; DALLENBACH et al., 2000). Atmospheric methane concentrations are high when temperatures are high. The timing and duration of the isotopic anomalies in the Bering Sea sediment cores are similar to the timing and duration of warm climate events that occurred during the last glacial period.

Table 1. Two samples, one with ordinary late Pleistocene isotopic values (1104 cm) and one with anomalous isotopic values (864 cm). We used the mean mass difference between the samples to estimate the isotopic composition of the authigenic overgrowths using a simple linear mixing model (see text).

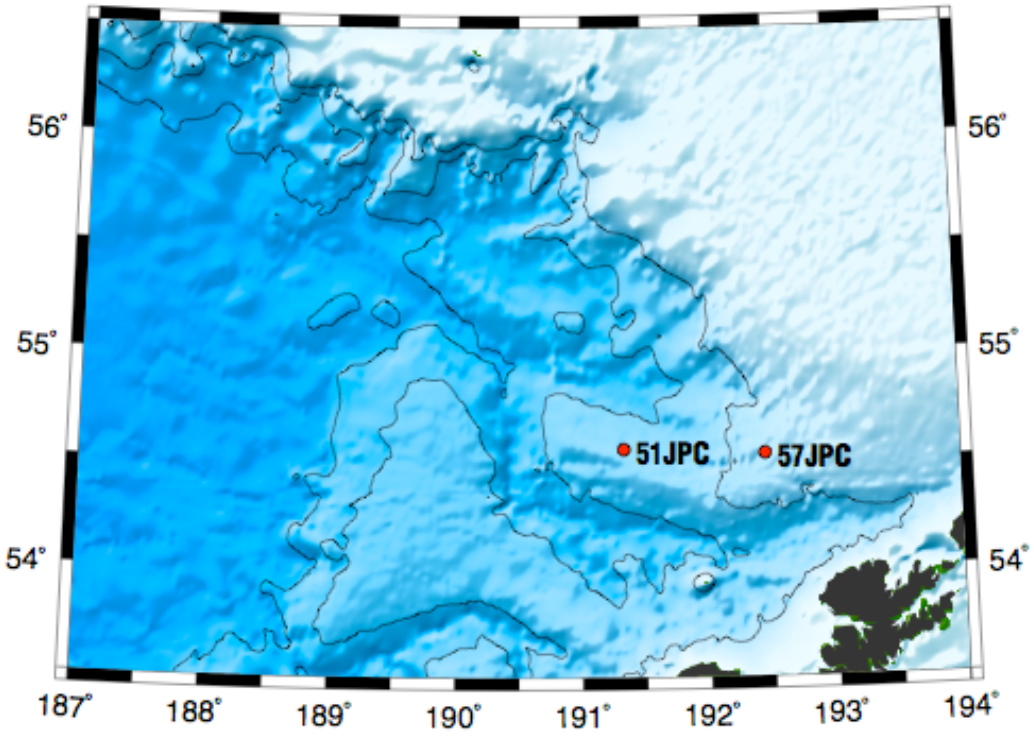

Figure 1

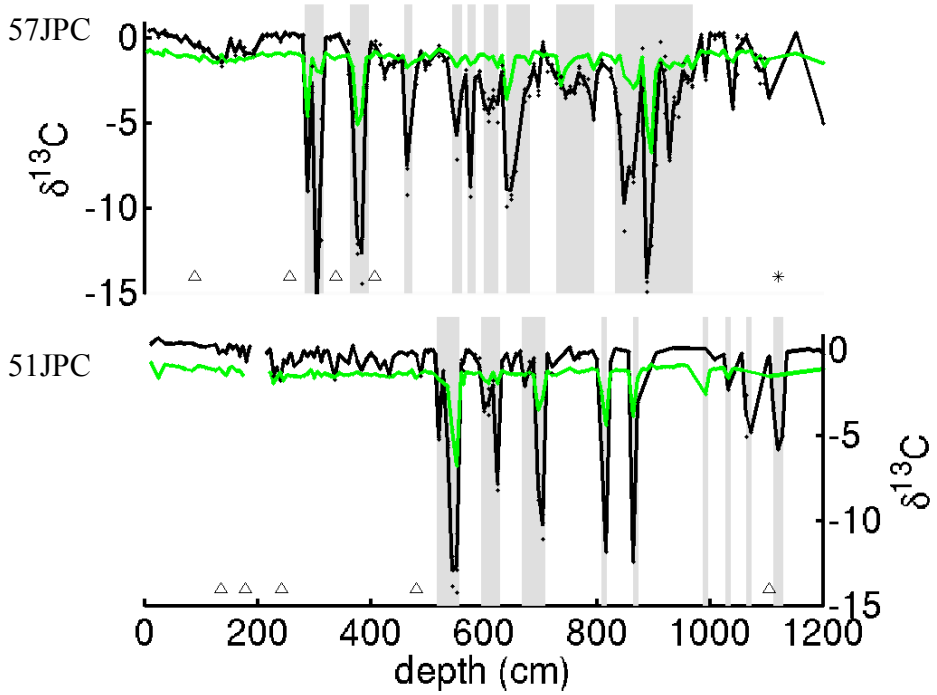

Figure 2

Figure 3

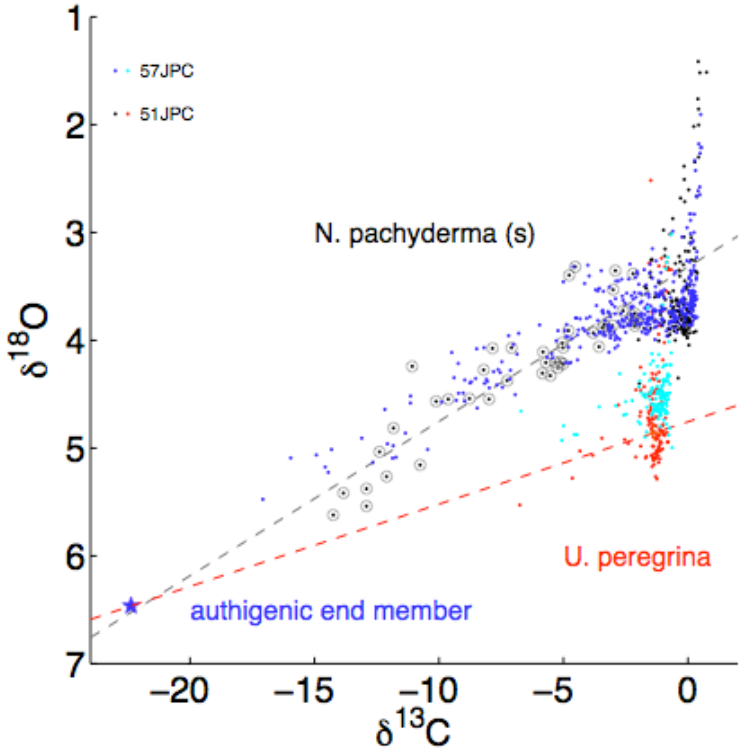

Figure 4

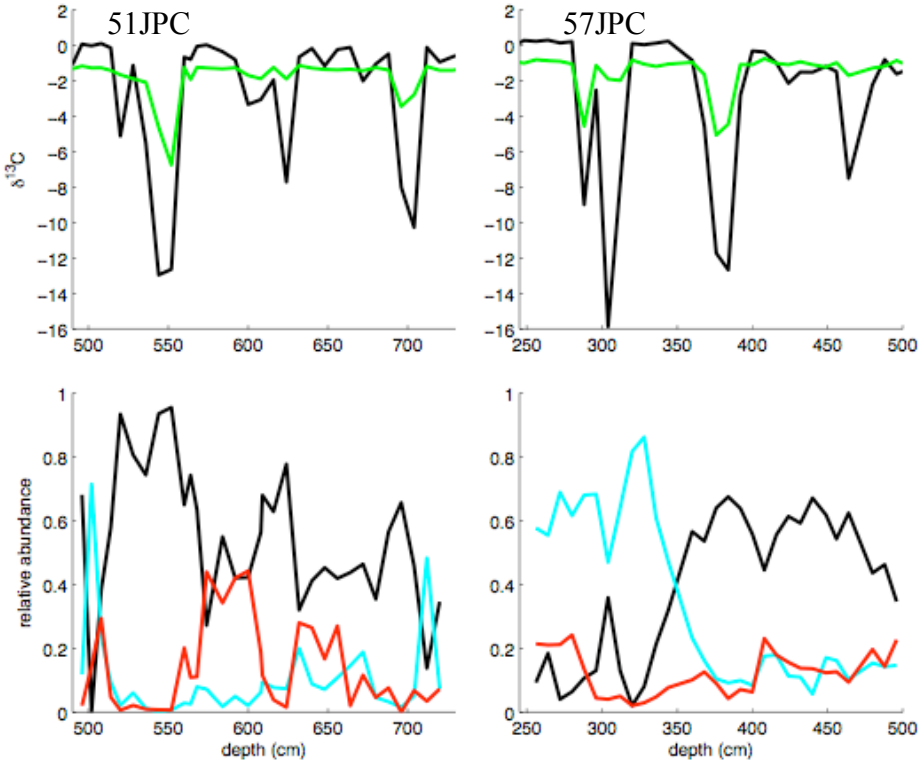

Figure 5

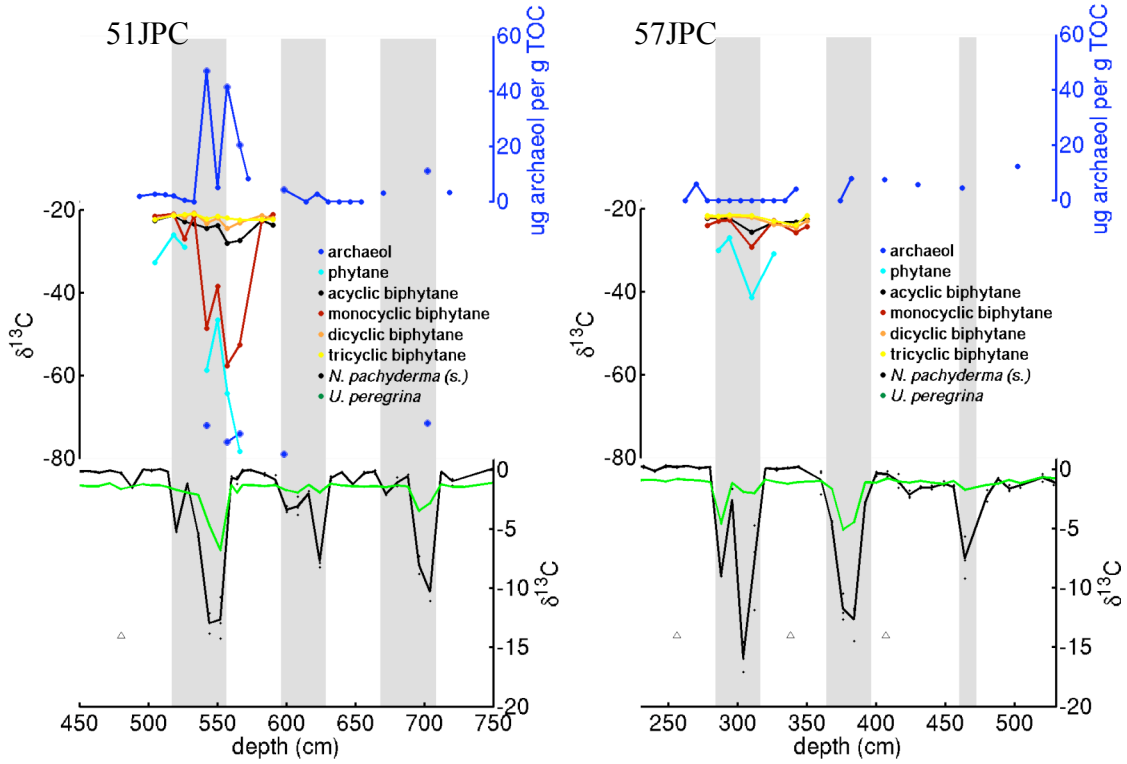

Figure 6

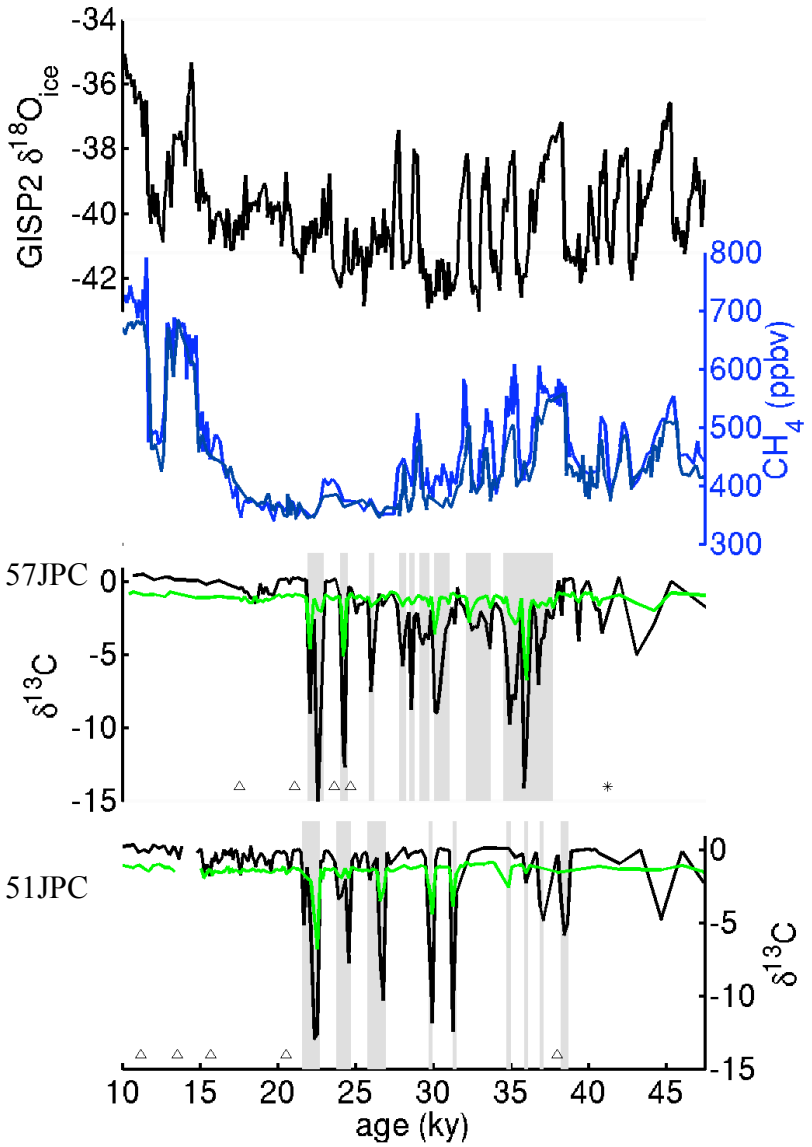

Figure 7

depth (cm)	#	mass (μg)	mean mass (μg)	$\delta^{13}C$ (‰)	$\delta^{18}O$ (‰)
864	40	212	5.3	–12.4	5.0
1104	40	97	2.4	–0.6	3.3

Table 1

6. REFERENCES

Berner, R. A., 1980. Early Diagenesis: a Theoretical Approach. Princeton University Press, Princeton, N.J.

Bhaumik, A. K. and Gupta, A. K., 2007. Evidence of methane release from Blake Ridge: ODP Hole 997A during the Plio-Pleistocene: benthic foraminifer fauna and total organic carbon. *Current Science* **92**, 192-199.

Blunier, T., Chappellaz, J., Schwander, J., Dällenbach, A., Stauffer, B., Stocker, T. F., Raynaud, D., Jouzel, J., Clausen, H. B., Hammer, C. U., and Johnson, S. J., 1998. Asynchrony of Antarctic and Greenland climate change during the last glacial period. *Nature* **394**, 739-734.

Brewer, P. G., Orr, F. M., Jr., Friederich, G., Kvenvolden, K. A., and Orange, D. L., 1998. Gas hydrate formation in the deep sea: In situ experiments with controlled release of methane, natural gas and carbon dioxide. *Energy and Fuels* **12**, 183-188.

Chappellaz, J., Barnola, J.-M., Raynaud, D., Korotkevich, Y. S., and Lorius, C., 1990. Ice-core record of atmospheric methane over the past 160,000 years. *Nature* **345**, 127-131.

Cook, M. S., Keigwin, L. D., and Sancetta, C. A., 2005. The deglacial history of surface and intermediate water of the Bering Sea. *Deep-Sea Research II* **52**, 2163-2173.

Dallenbach, A., Blunier, T., Fluckiger, J., Stauffer, B., Chappelaz, J., and Raynaud, D., 2000. Changes in the atmospheric CH4 gradient between Greenland and Antarctica during the last glacial and the transition to the Holocene. *Geophysical Research Letters* **27**, 1005-1008.

Davies, R. J. and Clark, I. R., 2006. Submarine slope failure primed and triggered by silica and its diagenesis. *Basin Research* **18**, 339-350.

Davies, R. J., Huuse, M., Hirst, P., Cartwright, J., and Yang, Y., 2006. Giant clastic intrusions primed by silica diagenesis. *Geology* **34**, 917-920.

de Garidel-Thoron, T., Beaufort, L., Bassinot, F., and Henry, P., 2004. Evidence for large methane releases to the atmosphere from deep-sea gas-hydrate dissociation during the last glacial episode. *Proceedings of the National Academy of Sciences* **101**, 9187-9192.

Dickens, G. R., O'Neil, J. R., Rea, D. K., and Owen, R. M., 1995. Dissociation of oceanic methane hydrate as a cause of the carbon-isotopic excursion at the end of the Paleocene. *Paleoceanography* **10**, 965-971.

Fritz, P. and Smith, D. G. W., 1970. The isotopic composition of secondary dolomites. *Geochimica et Cosmochimica Acta* **34**, 1161-1173.

Grootes, P. M. and Stuiver, M., 1997. Oxygen 18/16 variability in Greenland snow and ice with 1,000 to 100,000-year time resolution. *Journal of Geophysical Research* **102**, 26,455-26,470.

Hesselbo, S. P., Gröcke, D. R., Jenkyns, H. C., Bjerrum, C. J., Morgans Bell, H. S., and Green, O. R., 2000. Massive dissociation of gas hydrate during a Jurassic ocean anoxic event. *Nature* **406**, 392-395.

Hill, T. M., Kennett, J. P., Valentine, D. L., Yang, Z., Reddy, C. M., Nelson, R. K., Behl, R. J., Robert, C., and Beaufort, L., 2006. Climatically driven emissions of

hydrocarbons from marine sediments during deglaciation. *Proceedings of the National Academy of Sciences* **103**, 13570-13574.
Hinrichs, K.-U., Hmelo, L. R., and Sylva, S. P., 2003. Molecular fossil record of elevated methane levels in late Pleistocene coastal waters. *Science* **299**, 1214-1217.
Hoshiba, M., Ahagon, N., Ohkushi, K. i., Uchida, M., Motoyama, I., and Nishimura, A., 2006. Foraminiferal oxygen and carbon isotopes during the last 34 kyr off northern Japan, northwestern Pacific. *Marine Micropaleontology* **61**, 196-208.
Hughen, K., Lehman, S., Southon, J., Overpeck, J., Marchal, O., Herring, C., and Turnbull, J., 2004. ^{14}C Activity and Global Carbon Cycle Changes over the Past 50,000 Years. *Science* **303**, 202-207.
Johnsen, S. J., Dahl-Jensen, D., Gundestrup, N., Johnsen, S. J., Clausen, H. B., Dansgaard, W., Fuhrer, K., Gundestrup, N., Hammer, C. U., Iversen, P., Jouzel, J., Stauffer, B., and Steffensen, J. P., 1992. Irregular glacial interstadials recorded in a new Greenland ice core. *Nature* **359**, 311-313.
Johnsen, S. J., Dahl-Jensen, D., Gundestrup, N., Steffensen, J. P., Clausen, H. B., Miller, H., Masson-Delmotte, V., Sveinbjörnsdottir, A. E., and White, J., 2001. Oxygen isotope and palaeotemperature records from six Greenland ice-core stations: Camp Century, Dye-3, GRIP, GISP2, Renland and NorthGRIP. *Journal of Quaternary Science* **16**, 299-307.
Keigwin, L. D., 2002. Late Pleistocene-Holocene paleoceangraphy and ventilation of the Gulf of California. *Journal of Oceanography* **58**, 421-432.
Kennett, J. P., Cannariato, K. G., Hendy, I. L., and Behl, R. J., 2000. Carbon isotopic evidence for methane hydrate instability during Quaternary interstadials. *Science* **288**, 128-133.
Kennett, J. P., Cannariato, K. G., Hendy, I. L., and Behl, R. J., 2003. *Methane Hydrates in Quaternary Climate Change: the Clathrate Gun Hypothesis*. American Geophysical Union, Washington, D.C.
Klaucke, I., Sahling, H., Burk, D., Weinrebe, W., and Bohrmann, G., 2005. Mapping deep-water gas emissions with sidescan sonar. *EOS, Transactions, American Geophysical Union* **86**, 341.
Langworthy, T., 1986. Archaebacterial ether lipids and chemotaxonomy. *Systematic and applied microbiology* **7**, 253.
Lelieveld, J., Crutzen, P. J., and Bruhl, C., 1993. Climate effecs of atmospheric methane. *Chemosphere* **26**, 739-768.
Lembke, L., Tiedemann, R., Nürnberg, D., Biebow, N., and Kaiser, A., 2003. Benthic foraminiferal C-13 anomalies in the Okhotsk Sea: evidence for Holocene methane dissociation events. *EGS-AGU-EUG Joint Assembly, Abstracts from the meeting held in Nice, France, 6-11 April, 2003, abstract #10976*.
Lowry, A. R., 2006. Resonant slow falut slip in subduction zones forced by climatic load stress. *Nature* **442**, 802-805.
MacDonald, G. J., 1990. Role of methane clathrates in past and future climate. *Climatic Change* **16**, 247-281.
Maslin, M., Owen, M., Day, S., and Long, D., 2004. Linking continental-slope failures and climate change: testing the clathrate gun hypothesis. *Geology* **32**, 53-56.

McHugh, C. M., Ryan, W. B. F., and Schreiber, B. C., 1993. The role of diagenesis in exfoliation of submarine canyons. *American Association of Petroleum Geologists Bulletin* **77**, 145-172.

Mikaloff Fletcher, S. E., Tans, P. P., Bruhwiler, L. M., Miller, J. B., and Heimann, M., 2004. CH4 sources estimated from atmospheric observations of CH4 and its 13C/12C isotopic ratios: 1. Inverse modeling of source processes. *Global Biogeochemical Cycles* **18**, GB4004, doi:10.1029/2004GB002223.

Milkov, A. V., 2004. Global estimates of hydrate-bound gas in marine sediments: how much is really out there? *Earth Science Reviews* **66**, 183-197.

Millo, C., Sarnthein, M., and Erlenkeuser, H., 2005. Methane-driven late Pleistocene δ^13C minima and overflow reversals in the southwestern Greenland Sea. *Geology* **33**, 873-876.

Norris, R. D. and de Vargas, C., 2000. Evolution all at sea. *Nature* **405**, 23-24.

Orphan, V. J., Ussler, W., III, Naehr, T. H., House, C. H., Hinrichs, K.-U., and Paull, C. K., 2004. Geological, geochemical, and microbiological heterogeneity of the seafloor around methane vents in the Eel River Basin, offshore California. *Chemical Geology* **205**, 265-289.

Ostermann, D. R. and Curry, W. B., 2000. Calibration of stable isotopic data: an enriched δ^18O standard used for source gas mixing detection and correction. *Paleoceanography* **15**, 353-360.

Rau, G. H., Sweeny, R. E., and Kaplan, I. R., 1982. Plankton 13C-12C ratio changes with latitude: differences between northern and southern oceans. *Deep-Sea Research* **29**, 1035-1039.

Reimer, P. J., Baillie, M. G. L., Bard, E., Bayliss, A., Beck, J. W., Bertrand, C., Blackwell, P. G., Buck, C. E., Burr, G., Cutler, K. B., Damon, P. E., Edwards, R. L., Fairbanks, R. G., Friedrich, M., Guilderson, T. P., Hughen, K. A., Kromer, B., McCormac, F. G., Manning, S., Ramsey, C. B., Reimer, R. W., Remmele, S., Southon, J. R., Stuiver, M., Talamo, S., Taylor, F. W., van der Plicht, J., and Weyhenmeyer, C. E., 2004. Radiocarbon Calibration from 0-26 cal kyr BP. *Radiocarbon* **46**, 1029-1058.

Rubinstein, J. L., La Rocca, M., Vidale, J. E., Creager, K. C., and Wech, A. G., 2008. Tidal modulation of nonvolcanic tremor. *Science* **319**, 186-189.

Schmidt, M., Botz, R., Winn, K., Stoffers, P., Theissen, O., and Herzig, P., 2002. Seeping hydrocarbons and related carbonate mineralisations in sediments south of Lihir Island (Nwe Ireland forearc basin, Paupua New Guinea). *Chemical Geology* **186**, 249-264.

Shen, Z.-K., Wang, Q., Burgmann, R., Wan, Y., and Ning, J., 2005. Pole-tide modulation of slow slip events at circum-Pacific subduction zones. *Bulletin of the Seismological Society of America* **95**, 2009-2015.

Siddall, M., Rohling, E. J., Almogi-Labin, A., Hemleben, C., Meischner, D., Schmelzer, I., and Smeed, D. A., 2003. Sea-level fluctuations during the last glacial cycle. *Nature* **423**, 853-858.

Smith, L. M., Sachs, J. P., Jennings, A. E., Anderson, D. M., and deVernal, A., 2001. Light delta-13C events during deglaciation of the east Greenland continental shelf attributed to methane release from gas hydrates. *Geophysical Research Letters* **28**, 2217-2220.

Tarutani, T., Clayton, R. N., and Mayeda, T. K., 1969. The effect of polymorphism and magnesium substitution on oxygen isotope fractionation between calcium carbonate and water. *Geochimica et Cosmochimica Acta* **33**, 987-996.

Tsunogai, S., Kusakabe, M., Iizumi, H., Koike, I., and Hattori, A., 1979. Hydrographic features of the deep waters of the Bering Sea. *Deep-Sea Research* **26**, 641-659.

Uchida, M., Shibata, Y., Ohkushi, K. i., Ahagon, N., and Hoshiba, M., 2004. Episodic methane release events from last glacial marginal sediments in the western North Pacific. *Geochemistry Geophysics Geosystems* **5**, Q08005, doi:10.1029/2004GC000699.

Wakeham, S. G., Lewis, C. M., Hopmans, E. C., Schouten, S., and Damasté, J. S. S., 2003. Archaea mediate anaerobic oxidation of methane in deep euxinic waters of the Black Sea. *Geochimica et Cosmochimica Acta* **67**, 1359-1374.

Wefer, G., Heinze, P.-M., and Berger, W. H., 1994. Clues to ancient methane release. *Nature* **369**, 282.

Wiedicke, M. and Weiss, W., 2006. Stable carbon isotope records of carbonates tracing fossil seep activity off Indonesia. *Geochemistry Geophysics Geosystems* **7**, Q11009, doi:10.1029/2006GC001292.

Williams, L. A. and Crerar, D. A., 1985. Silica Diagenesis, II. General Mechanisms. *Journal of Sedimentary Petrology* **55**, 312-321.

Williams, L. A., Parks, G. A., and Crerar, D. A., 1984. Silica diagenesis, I. Solubility Controls. *Journal of Sedimentary Petrology* **55**, 301-311.

7. LIST OF ACRONYMS AND ABBREVIATIONS

ppbv	parts per billion by volume
Tg/y	10^{12} g per year
GDGT	glyceryl dibiphytanyl glyceryl tetraether\
$\delta^{13}C$	$1000\left(\frac{^{13}C/^{12}C_{sample}}{^{13}C/^{12}C_{standard}}-1\right)$
$\delta^{18}O$	$1000\left(\frac{^{18}O/^{16}O_{sample}}{^{18}O/^{18}O_{standard}}-1\right)$
VPDB	Vienna Peedee Belemnite
AMS	accelerator mass spectrometer
ΔR	the local anomaly from the global mean of ^{14}C age of sea surface water
TLE	total lipid extract
v/v	volume/volume
TMS	trimethylsilyl
GC	gas chromatograph
MS	mass spectrometer
LGM	Last Glacial Maximum
‰	parts per thousand
DO	Dansgaard-Oeschger
opal A	biogenic silica
opal CT	cristobalite and tridymite